Free Radical Research, March 2007; 41(3): 295–302

The reactivity of carotenoid radicals with oxygen

ALI EL-AGAMEY[1,2] & DAVID J. McGARVEY[1]

[1]*School of Physical and Geographical Sciences, Lennard-Jones Laboratories, Keele University, Keele, Staffordshire, ST5 5BG, UK, and* [2]*Chemistry Department, Faculty of Science, New Damietta, Egypt*

Accepted by Professor H. Sies

(Received 13 July 2006; in revised form 10 August 2006)

Abstract
The possibility that carotenoid radicals react with oxygen to form chain-carrying peroxyl radicals has been postulated to account for the reduction in antioxidant effetiveness displayed by some carotenoids at high oxygen concentrations. The primary objective of the work described in this paper was to measure the rate constants for oxygen addition to a series of carotenoid radicals and to examine any influence of carotenoid structural features on these rate constants. Laser flash photolysis has been used to generate long-lived carotenoid radicals ($PhS-CAR^{\cdot}$) derived from radical addition reactions with phenylthiyl radicals ($PhS^{\cdot}$) in benzene. The $PhS-CAR^{\cdot}$ radicals are scavenged by oxygen at rates that display a moderate dependence on the number of conjugated double bonds (n_{db}) in the carotenoid. The rate constants range from $\sim 10^3$ to $\sim 10^4\,M^{-1}\,s^{-1}$ for $n_{db} = 7-11$. The data also suggest that the presence of terminal cyclic groups may cause an increase in the rate constant for oxygen addition.

Keywords: *Carotenoids, carotenoid radicals, antioxidants, thiyl radicals, peroxyl radicals, laser flash photolysis*

Introduction

In non-polar (lipophilic) environments carotenoids appear to react with a range of free radicals ($R^{\cdot}$) via addition to the polyene chain (equation (1)), producing an uncharged resonance-stabilised carotenoid addition radical ($R\text{-}CAR^{\cdot}$) [1,2]. However, allylic H-atom abstraction from methyl groups (for example, at positions 5, 9, 13 in the case of β-carotene) [3] is also possible. In addition, carotenoids such as β-carotene appear to be particularly vulnerable to allylic H-atom abstraction from position 4 and there is evidence that such reactions play a role in carotenoid anti-oxidant chemistry [4].

$$R^{\cdot} + CAR \rightarrow R-CAR^{\cdot} \qquad (1)$$

Our recent results from time-resolved studies of the reactions of carotenoids with thiyl radicals ($RS^{\cdot}$) [1,5–7] and acylperoxyl radicals ($AcylOO^{\cdot}$) [2,8] suggest that radical scavenging occurs via addition and indicate that the carotenoid addition radicals formed in these reactions absorb in the visible region [1,2,5], close to the region of the parent carotenoid absorption bands. This is consistent with results of recent theoretical calculations (ZINDO/S) of the electronic absorption spectra of uncharged carotenoid radicals, which predict absorption bands in the visible region and also that the absorption maximum increases with the number of delocalised π-electrons in the carotenoid radical (for example, the predicted absorption maxima for β-carotene-derived radicals with 15, 19 and 23 delocalised π-electrons are 438, 504 and 549 nm, respectively) [3].

Our recent work on carotenoid free radical chemistry has focused on the reactions of carotenoids with $AcylOO^{\cdot}$ and $PhS^{\cdot}$ radicals and in particular, the

---

Correspondence: D. J. McGarvey, School of Physical and Geographical Sciences, Lennard-Jones Laboratories, Keele University, Keele, Staffordshire, ST5 5BG, UK. Fax: 44 1782 712378. E-mail: d.j.mcgarvey@chem.keele.ac.uk

ISSN 1071-5762 print/ISSN 1029-2470 online © 2007 Informa UK Ltd.
DOI: 10.1080/10715760601087558

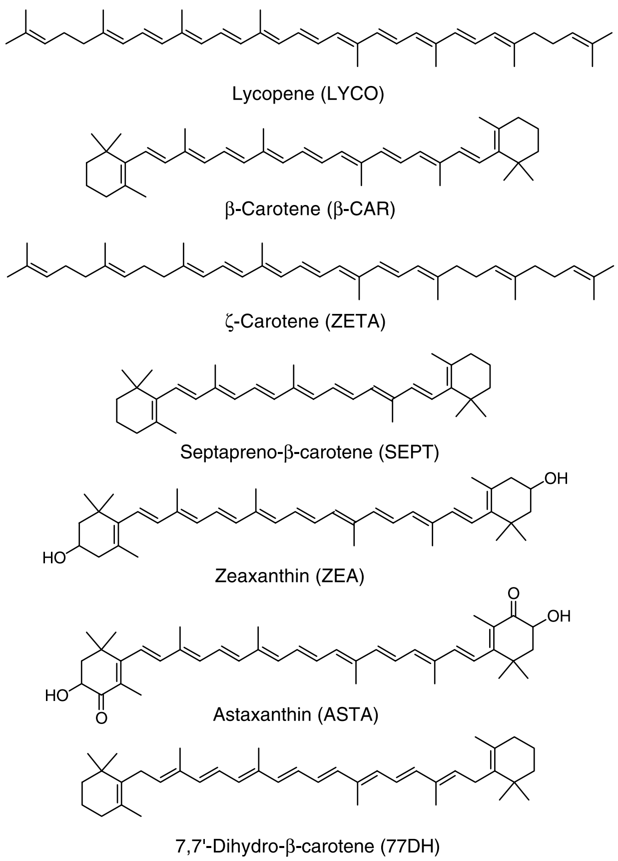

Figure 1. Structures of carotenoids.

properties of the resulting carotenoid addition radicals. In the case of the retro carotenoid 7,7′-dihydro-β-carotene (77DH, Figure 1), the R-77DH˙ addition radicals display intense absorption bands (peaking at ~455–470 nm depending on the solvent, see Figure 2) that are well separated from the parent 77DH absorption. Radical addition at one of the terminal positions of 77DH yields a carotenoid radical with 15 delocalised π-electrons and the positions of the experimentally observed R-77DH˙ absorption bands are in reasonable agreement with theoretical calculations [3] (see above). Indeed, part of the evidence that radical addition is favoured over allylic H-atom abstraction is that the 77DH radicals formed from reaction with AcylOO˙ radicals and PhS˙ radicals have similar absorption spectra, but very different decay kinetics (the radicals derived from reaction with AcylOO˙ radicals decay relatively rapidly (tens of μs) by 1st order kinetics, probably due to an intramolecular process leading to epoxide formation [2], whilst the radicals derived from reaction with PhS˙ radicals persist for tens of ms, see Figure 2). If reactions with both AcylOO˙ and PhS˙ radicals proceeded via allylic H-atom abstraction then it would be expected that the resulting 77DH radicals would exhibit not only similar spectra, but also similar decay kinetics.

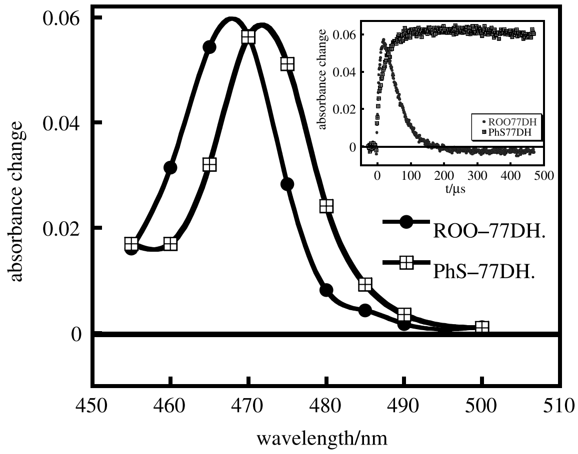

Figure 2. Comparison of the absorption spectra (normalised) and decay kinetics (inset) of the addition radicals AcOO–77DH˙ and PhS–77DH˙ in benzene.

In the context of anti-oxidant chemistry, there is considerable interest in the reactivity of anti-oxidant derived radicals towards oxygen and the factors that influence this reactivity [9–13]. In a much cited paper, Burton and Ingold [14] invoked the reversible reaction of carotenoid radicals (R-CAR˙) with oxygen, forming potential chain-carrying peroxyl radicals (R-CAR-OO˙), to account for the reduced effectiveness of β-carotene as an antioxidant at elevated oxygen concentrations (Scheme 1). However, it was not until recently that such reactions involving carotenoid radicals have actually been directly observed [1].

$$\mathrm{R}^{\bullet} + \mathrm{CAR} \longrightarrow \mathrm{R\text{-}CAR}^{\bullet} + \mathrm{O_2} \rightleftharpoons \mathrm{R\text{-}CAR\text{-}OO}^{\bullet}$$

Scheme 1.

We previously attempted to investigate the reaction of oxygen with AcylOO–77DH˙ radicals [2], formed by reaction of 77DH with AcylOO˙ radicals, but were unable to observe any influence of oxygen on the decay of AcylOO–77DH˙. However, as explained above, the intrinsic decay of these radicals (Figure 2) is relatively rapid and it is now clear that the failure to observe any reaction with oxygen simply reflects the fact that $k_1 \ggg k_q[\mathrm{O_2}]$ in this case (Scheme 2 and Figure 2). The competition between the intrinsic decay of R-CAR˙ to non-radical products and its reaction with oxygen to form R-CAR-OO˙ is likely to be a significant factor in determining the antioxidant properties of carotenoids within a specified system subjected to free-radical mediated oxidation.

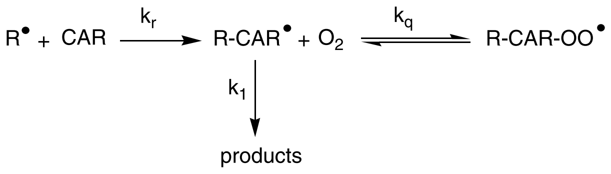

$$\mathrm{R}^{\bullet} + \mathrm{CAR} \xrightarrow{k_r} \mathrm{R\text{-}CAR}^{\bullet} + \mathrm{O_2} \overset{k_q}{\rightleftharpoons} \mathrm{R\text{-}CAR\text{-}OO}^{\bullet};\quad \mathrm{R\text{-}CAR}^{\bullet} \xrightarrow{k_1} \text{products}$$

Scheme 2.

The relatively long lifetimes of the PhS–CAR$^{\cdot}$ addition radicals makes it possible to observe their reactions with oxygen and to measure the reaction rate constant. Our initial measurements for 77DH and β-carotene were reported recently [1]. In the work reported here, we have extended these measurements to include a range of carotenoid radicals derived from reactions of PhS$^{\cdot}$ with lycopene (LYCO), ζ-carotene (ZETA), septapreno-β-carotene (SEPT), zeaxanthin (ZEA) and astaxanthin (ASTA). The results are discussed in terms of the variation of the oxygen addition rate constant with the degree of resonance-stabilisation in the PhS–CAR$^{\cdot}$ addition radical.

Materials and methods

Materials

Benzene (Aldrich, HPLC grade) and phenyl disulphide (Fluka) were used as received. The carotenoids were kindly supplied by DSM Nutritional Products and used as received. Oxygen (1, 5, 50 (balance nitrogen) and 100%) and argon were supplied by the British Oxygen Company.

Experimental methods

The details of the laser flash photolysis system have been described previously [15]. Unless otherwise stated, 355 nm laser energies were in the range 1–5 mJ pulse^{-1} with a beam diameter of ~4 mm. Quartz sample cells (2 mm excitation pathlength × 10 mm monitoring pathlength) fitted with vacuum taps (where necessary) were employed for the laser flash photolysis measurements. If necessary, (for example, during acquisition of transient absorption spectra) fresh solution was introduced into the sample cell following each exposure to the laser.

Results

Laser photolysis (355 nm) of phenyl disulphide (PhS–SPh) in benzene gives rise to PhS$^{\cdot}$ radicals, which exhibit a broad absorption band in the 400–500 nm region and decay by second order kinetics (equation (2)). The decay of PhS$^{\cdot}$ is not influenced by oxygen [1,16] in the range of oxygen concentrations used in this study (up to ~0.01 M).

$$\mathrm{PhS{-}SPh} \overset{h\nu}{\rightleftarrows} 2\,\mathrm{PhS}^{\cdot} \qquad (2)$$

Lycopene (LYCO)

Laser photolysis (355 nm) of air-saturated benzene solutions of 8×10^{-3} M PhS–SPh in the presence of 1.3×10^{-5} M LYCO leads to the formation (on a microsecond timescale) of an intense transient visible absorption band around 545 nm (Figure 3A) attributed to PhS–LYCO$^{\cdot}$ (equation (3)). No transient absorption features were observed at longer wavelengths in the visible or near infrared regions.

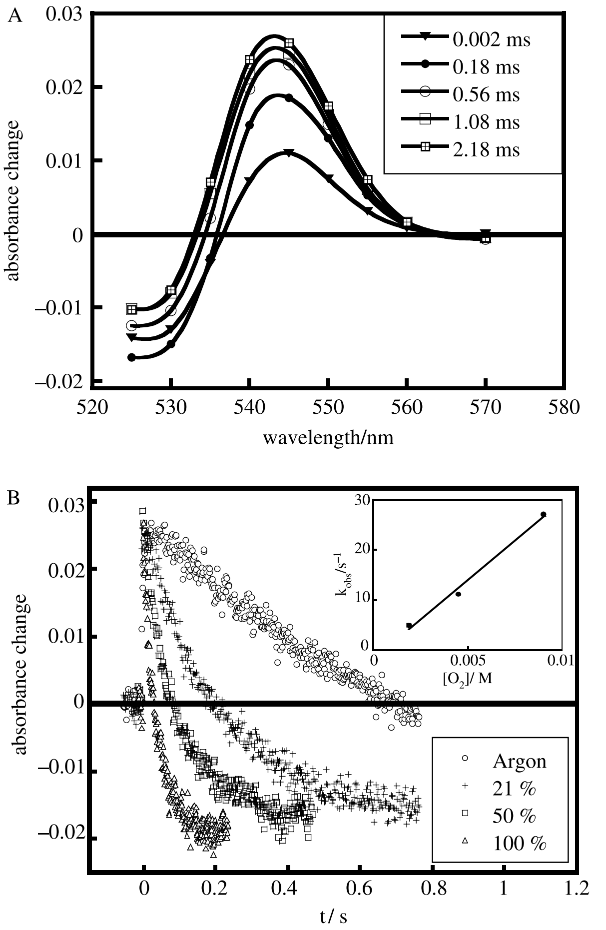

Figure 3. (A) Transient spectra of PhS–LYCO$^{\cdot}$ obtained following 355 nm laser photolysis of PhS–SPh (8×10^{-3} M) in the presence of LYCO (1.3×10^{-5} M) in benzene (air saturated, laser energy = 1.5 mJ). (B) Normalized kinetic absorption profiles, at 293 K, for the decay of PhS–LYCO$^{\cdot}$ at 545 nm in benzene at various oxygen concentrations. The inset shows a plot of the room temperature pseudo-first order rate constant (k_{obs}) for the decay of PhS–LYCO$^{\cdot}$ (at 545 nm) in benzene versus the oxygen concentration.

$$\mathrm{PhS}^{\cdot} + \mathrm{LYCO} \rightarrow \mathrm{PhS{-}LYCO}^{\cdot} \qquad (3)$$

In the absence of oxygen, PhS–LYCO$^{\cdot}$ persists for several 100 ms under our experimental conditions. As the oxygen concentration is increased the decay rate increases progressively and this is accompanied by increased bleaching at longer times (see Figure 3B). The decay in the presence of oxygen is exponential and the observed pseudo 1st order rate constant (k_{obs}) can be expressed by equation (4).

$$k_{obs} = k_1 + k_q[O_2] \qquad (4)$$

A plot of k_{obs} versus $[O_2]$ (equation (4)) allows extraction of the rate constant (k_q) for oxygen addition of $3.16 \pm 0.31 \times 10^3\,\mathrm{M^{-1}\,s^{-1}}$ from the slope of the linear graph (see inset of Figure 3B). The rate constant is smaller (by a factor of ~2) than that determined previously for PhS–β-CAR$^{\cdot}$ ($6.4 \pm 0.9 \times 10^3\,\mathrm{M^{-1}\,s^{-1}}$) [1]. Assuming terminal addition of PhS$^{\cdot}$ in both cases then the extent of the delocalised π-system should be the same and consequently the rate constant for oxygen addition would be anticipated to be very similar. The observed difference could be due to the fact that the double bonds in the terminal cyclic rings of β-CAR do not lie co-planar with the rest of the conjugated system and this effect may persist in PhS–β-CAR$^{\cdot}$, resulting in a slightly lower degree of resonance stabilisation and consequently a larger rate constant for oxygen addition than for PhS–LYCO$^{\cdot}$ [4,17]. Alternatively, radical addition to β-CAR may occur at the first double bond within the main polyene chain, rather than at one of the double bonds within the terminal rings, leading to a resonance-stabilised radical with fewer de-localised π-electrons. For reasons associated with spectral overlap of the addition radical absorption with the parent carotenoid absorption, we are unable to establish whether or not oxygen addition is reversible under our experimental conditions.

ζ-Carotene (ZETA)

Laser photolysis (355 nm) of benzene solutions of 8×10^{-3} M PhS–SPh in the presence of 2.6×10^{-5} M ZETA leads to the formation (on a microsecond timescale) of a transient visible absorption band around 455 nm (Figure 4A) attributed to PhS–ZETA$^{\cdot}$ (equation (5)). No transient absorption features were observed at longer wavelengths in the visible or near infrared regions.

$$\mathrm{PhS^{\cdot} + ZETA \rightarrow PhS{-}ZETA^{\cdot}} \qquad (5)$$

Figure 4B shows the effect of increasing oxygen concentration on the decay of PhS–ZETA$^{\cdot}$. Analysis of the variation of k_{obs} with [O$_2$] in an analogous manner to that described above for LYCO leads to a rate constant (k_q) for oxygen addition of $3.44 \pm 0.4 \times 10^4\,\mathrm{M^{-1}\,s^{-1}}$ (Figure 4B). ZETA and LYCO have the same hydrocarbon backbone and the higher value of k_q for ZETA, relative to that for LYCO, probably reflects the lower degree of resonance stabilisation present in PhS–ZETA$^{\cdot}$ relative to PhS–LYCO$^{\cdot}$. As for LYCO, at present we are unable to establish whether the oxygen addition is reversible.

Septapreno-β-carotene (SEPT)

Laser photolysis (355 nm) of benzene solutions of 0.025 M PhS–SPh in the presence of 1.4×10^{-4} M SEPT leads to the formation (on a microsecond timescale) of a visible absorption band around 495 nm (Figure 5A) attributed to PhS–SEPT$^{\cdot}$ (equation (6)). No transient absorption features were observed at longer wavelengths in the visible or near infrared regions. A higher carotenoid concentration was used in the case of SEPT because the absorption of the additional radical is weaker than that for other carotenoids such as LYCO and ZETA. Also, it is notable that the intrinsic decay of PhS–SEPT$^{\cdot}$ is considerably faster than that exhibited by PhS–LYCO$^{\cdot}$ and PhS–ZETA$^{\cdot}$ which may be due to reaction of PhS–SEPT$^{\cdot}$ with the parent carotenoid (Figure 5B).

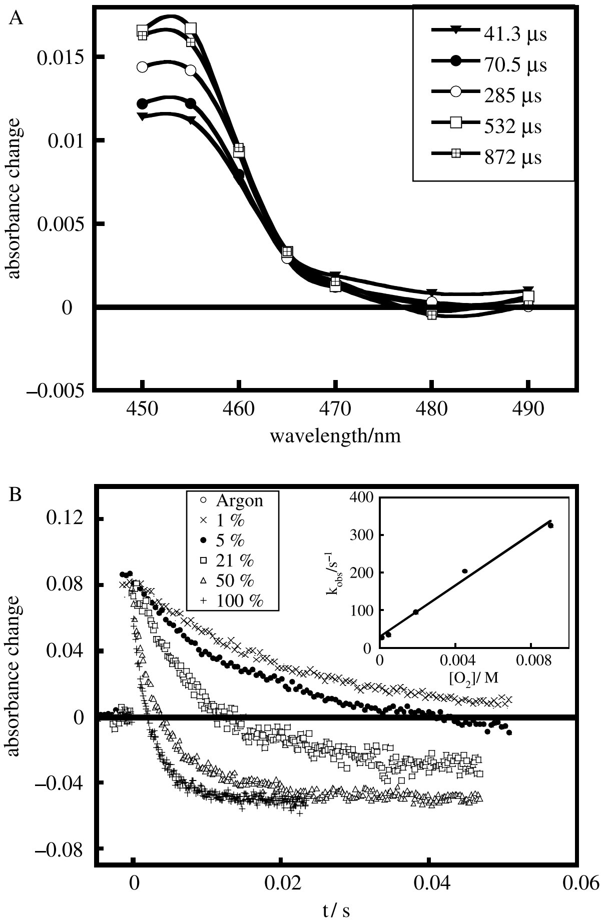

Figure 4. (A) Transient spectra of PhS–ZETA$^{\cdot}$ obtained following 355 nm laser photolysis of PhS–SPh (8×10^{-3} M) in the presence of ZETA (2.6×10^{-5} M) in benzene (air saturated, laser energy = 1.5 mJ). (B) Normalized kinetic absorption profiles, at 293 K, for the decay of PhS–ZETA$^{\cdot}$ at 455 nm in benzene at various oxygen concentrations (laser energy = 5 mJ). The inset shows a plot of the room temperature pseudo-first order rate constant (k_{obs}) for the decay of PhS–ZETA$^{\cdot}$ (at 455 nm) in benzene versus the oxygen concentration.

$$\mathrm{PhS^{\cdot} + SEPT \rightarrow PhS{-}SEPT^{\cdot}} \qquad (6)$$

Figure 5B shows the effect of increasing oxygen concentration on the decay of PhS–SEPT$^{\cdot}$. Analysis of the variation of k_{obs} with [O$_2$], as before, leads to a rate constant (k_q) for oxygen addition of $3.5 \pm 1.5 \times 10^4\,\mathrm{M^{-1}\,s^{-1}}$ (Figure 5B). The larger error

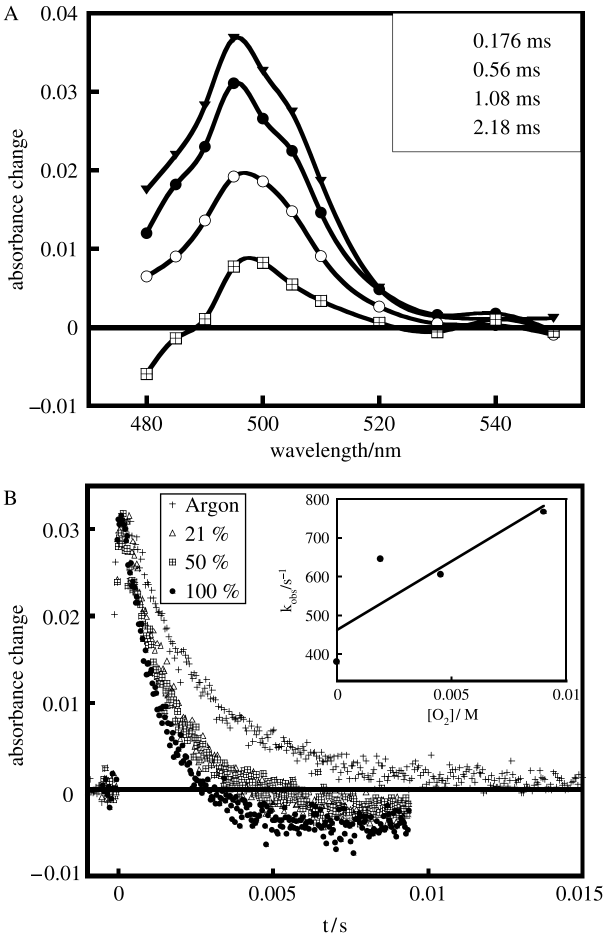

Figure 5. (A) Transient spectra of PhS–SEPT$^{\cdot}$ obtained following 355 nm laser photolysis of PhS–SPh (0.025 M) and SEPT (1.4×10^{-4} M) in benzene (air saturated, laser energy = 4 mJ). (B) Normalized kinetic absorption profiles, at 293 K, for the decay of PhS–SEPT$^{\cdot}$ at 500 nm in benzene at various oxygen concentrations. The inset shows a plot of the room temperature pseudo-first order rate constant (k_{obs}) for the decay of PhS–SEPT$^{\cdot}$ (at 500 nm) in benzene versus the oxygen concentration.

margin on this value reflects the relatively fast intrinsic decay of PhS–SEPT$^{\cdot}$ under the conditions used.

Zeaxanthin (ZEA)

Laser photolysis (355 nm) of benzene solutions of 8×10^{-3} M PhS–SPh in the presence of 5.7×10^{-5} M ZEA leads to the formation (on a microsecond timescale) of a weak visible absorption band around 540 nm (Figure 6A) attributed to PhS–ZEA$^{\cdot}$ (equation (7)). No transient absorption features were observed at longer wavelengths in the visible or near infrared regions. A higher carotenoid concentration was used here for the same reasons already explained for SEPT.

$$\mathrm{PhS^{\cdot} + ZEA \rightarrow PhS{-}ZEA^{\cdot}} \qquad (7)$$

Figure 6B shows the effect of increasing oxygen concentration on the decay of PhS–ZEA$^{\cdot}$. Analysis of the variation of k_{obs} with [O$_2$], as before, leads to a rate constant (k_q) for oxygen addition of $1.1 \pm 0.5 \times 10^{4}\,\mathrm{M^{-1}\,s^{-1}}$ (Figure 6B). The large error margin reflects the relatively fast intrinsic decay of PhS–ZEA$^{\cdot}$.

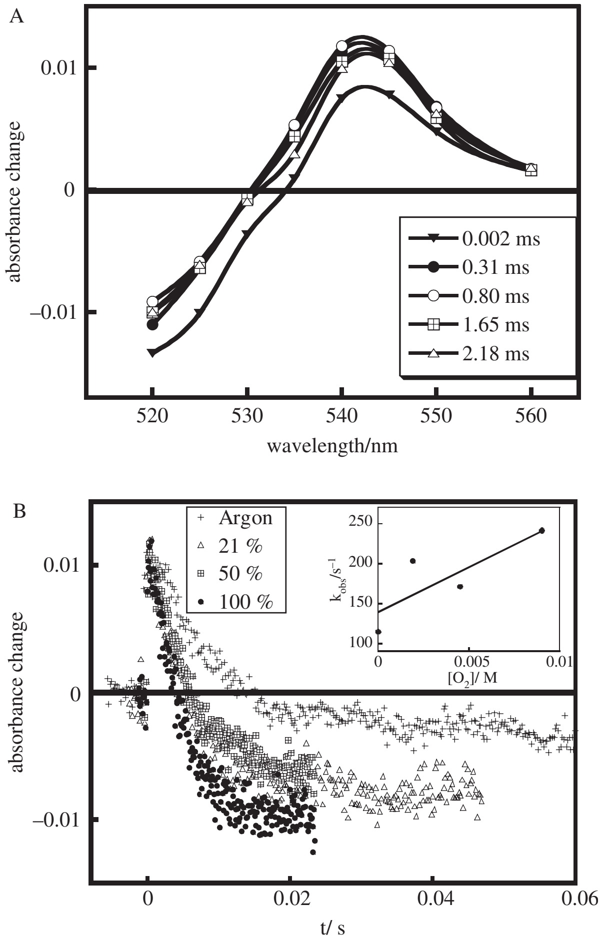

Figure 6. (A) Transient spectra of PhS–ZEA$^{\cdot}$ obtained following 355 nm laser photolysis of PhS–SPh (8×10^{-3} M) and ZEA (5.7×10^{-5} M) in benzene (air saturated, laser energy = 4.5 mJ). (B) Normalized kinetic absorption profiles, at 293 K, for the decay of PhS–ZEA$^{\cdot}$ at 540 nm in benzene at various oxygen concentrations (laser energy = 4 mJ). The inset shows a plot of the room temperature pseudo-first order rate constant (k_{obs}) for the decay of PhS–ZEA$^{\cdot}$ (at 540 nm) versus the oxygen concentration.

Astaxanthin (ASTA)

Laser photolysis (355 nm) of benzene solutions of 8×10^{-3} M PhS–SPh in the presence of 8.7×10^{-5} M ASTA shows only bleaching in the ASTA ground state absorption and does not give any resolved bands beyond the ASTA ground state absorption range (Figure 7). This bleaching could be attributed to the formation of PhS–ASTA$^{\cdot}$, which absorbs in the same region as ASTA (equation (8)), but less strongly.

$$\mathrm{PhS^{\cdot} + ASTA \rightarrow PhS{-}ASTA^{\cdot}} \qquad (8)$$

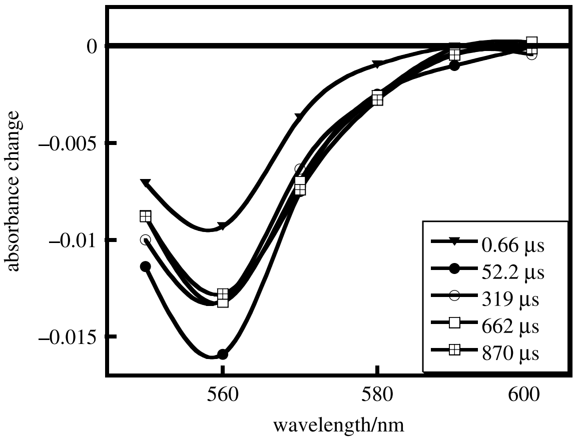

Figure 7. Transient spectra obtained following laser photolysis of PhS–SPh (8×10^{-3} M) in the presence of ASTA (8.7×10^{-5} M) in benzene (air saturated, laser energy = 4.5 mJ).

Discussion

Trends in oxygen addition rates

Oxygen additions to carbon-centred radicals are often diffusion-controlled ($\sim 10^9\,M^{-1}\,s^{-1}$) [18]. However, increased resonance-stabilisation of carbon-centred radicals leads to a reduction in the rate constant for oxygen addition [9–13]. In polyene systems, this reduction in the observed rate constant for oxygen addition partly reflects the fact that various non-terminal oxygen additions are rendered ineffective because the reverse reaction (loss of oxygen to regenerate the carbon-centred radical) for such peroxyl radicals is very fast [19–22] relative to that for peroxyl radicals derived from terminal oxygen addition. In other words, the probability that oxygen makes successful encounters at terminal positions decreases as the extent of the resonance stabilisation increases. This scenario is summarised in Scheme 3 for oxygen addition to carotenoid radicals.

We have previously presented evidence [1] for the reversibility of oxygen addition to PhS–77DH˙. However, the absorption band for PhS–77DH˙ is well resolved from the parent 77DH absorption which simplifies the analysis of the experimental data in terms of the reversibility of oxygen addition. Unfortunately, this is not the case for the other carotenoids studied in this work, all of which show bleaching of the parent carotenoid absorption in the presence of oxygen (this bleaching increases as the oxygen concentration is increased, see Figures 3B, 4B, 5B and 6B). The absorption changes associated with the parent carotenoid, which overlap the absorption changes due to the carotenoid radical, make analysis of the reversibility of the reactions very complicated and consequently, we are currently unable to draw any conclusions concerning the reversibility of oxygen addition for these carotenoid radicals. In addition, secondary reactions of the carotenoid peroxyl radicals (R-CAR-OO˙) may compete with the reverse step (loss of oxygen).

The results for the rates of oxygen addition to carotenoid radicals are summarised in Table I. It is apparent that the oxygen addition rate constants generally decrease with the number of conjugated double bonds in the parent carotenoid. However, this dependence is not a strong one and the variation

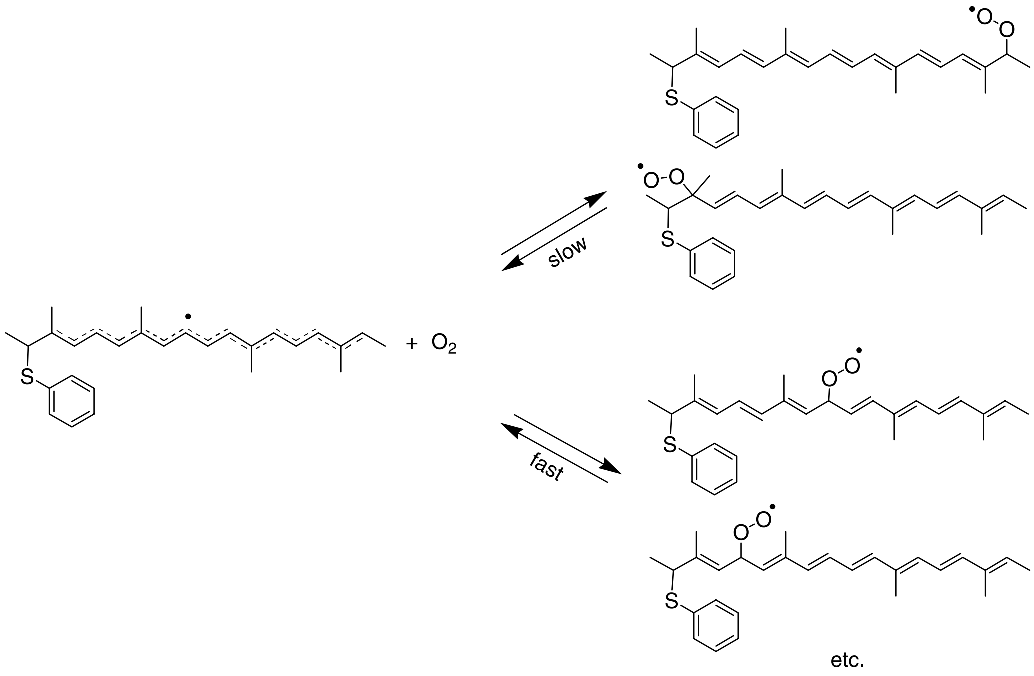

Scheme 3.

Table I. The rate constants (k_q) for the reaction of carotenoid neutral radical (PhS–CAR$^\bullet$) with oxygen and the λ_{max} of PhS–CAR$^\bullet$ in benzene.

CAR	n_{db}*	k_q ($10^4\,M^{-1}\,s^{-1}$)	λ_{max} (nm)
ZETA	7	3.44 ± 0.4	455
77DH	8	4.3 ± 0.07 [1]	470
SEPT	9	3.5 ± 1.5	500
β-CAR	11	0.64 ± 0.09 [1]	540
LYCO	11	0.32 ± 0.03	545
ZEA	11	1.1 ± 0.5	540
ASTA	13	–	–

* n_{db} is the number of conjugated double bonds in the parent carotenoid.

in k_q is not more than one order of magnitude. Within the error margins of the measurements, the three carotenoids with 7, 8 and 9 conjugated double bonds respectively have similar rate constants for oxygen addition ($\sim 3–4 \times 10^4\,M^{-1}\,s^{-1}$). In the case of LYCO and β-CAR with 11 double bonds, the oxygen addition rate constants are significantly smaller ($0.32 \times 10^4\,M^{-1}\,s^{-1}$ and $0.64 \times 10^4\,M^{-1}\,s^{-1}$, respectively) and the difference between the rate constants for LYCO and β-CAR may reflect the influence of the terminal cyclic rings as discussed earlier (see results section). The rate constant obtained for ZEA is out of step and somewhat larger than for LYCO and β-CAR. However, the error margins in the rate constant for ZEA are larger due principally to the fast intrinsic decay of the PhS–ZEA$^\bullet$ radical under the experimental conditions used. The rapid intrinsic decay of the radical means that the observed effect of oxygen on its decay is less marked, leading to a significantly larger uncertainty in the determined oxygen addition rate constant. Thus, in the case of PhS–ZEA$^\bullet$, we can only say that the oxygen addition rate constant is in the same range as for LYCO and β-CAR. We are currently investigating alternative approaches to the determination of oxygen addition rate constants in order to overcome some of the challenges, we have encountered in making these measurements for some carotenoids (e.g. ASTA, ZEA).

Relevance to the antioxidant properties of carotenoids

The radical scavenging antioxidant properties of carotenoids are well documented [6,23–25] as are some of the mechanistic details of the free radical chemistry involved [2,24]. However, kinetic data relating to the rate constants of the various elementary reactions is comparatively sparse and such data are required if the variations in the antioxidant properties of carotenoids with various system parameters (oxygen concentration, carotenoid structure, etc.) are to be fully understood [26,27].

The free-radical scavenging antioxidant properties displayed by carotenoids are partly dependent upon the competition between the intrinsic decay of the initially formed carotenoid-derived free radicals and their reactions with oxygen (Scheme 2). We have shown that the intrinsic decay of some carotenoid addition radicals (particularly AcylOO–CAR$^\bullet$, derived from reactions with acylperoxyl radicals [2]) can compete effectively with oxygen addition. However, the rate constant for the intrinsic decay of carotenoid radical may vary markedly depending on, for example, the nature of the scavenged radical and the properties of the environment (e.g. polarity). Hence, the reaction channel distribution between intrinsic decay and oxygen addition will depend on the nature of the scavenged radical, the nature of the carotenoid, the solvent and the oxygen concentration in the system under study. This is an area that requires further investigation.

The addition of oxygen to carotenoid radicals has been invoked previously to account for the observed reduction in antioxidant effectiveness of some carotenoids at high oxygen concentrations [23,26,28–31] and has been identified as a key reaction in the context of the antioxidant properties of carotenoids [27,29]. Palozza et al. [30] studied the antioxidant/pro-oxidant role of β-CAR in murine normal and tumor thymocytes and demonstrated the strong influence of oxygen tension on the antioxidant effectiveness of β-CAR. More recently, Tesoriere et al. [32] in a study of antioxidant reactions of retinol in phosophlipid bilayers, showed that besides free radical trapping, consumption of retinol during lipid oxidation occurs via self-oxidation reactions that are retinol concentration and oxygen concentration dependent. In addition, Vile and Winterbourn [33] in a study of the antioxidant effectiveness of β-CAR and retinol toward adriamycin-promoted microsomal lipid peroxidation showed that the inhibition of lipid peroxidation by β-CAR is oxygen concentration dependent, whilst for retinol it is not. Of course there are many factors (e.g. orientation and location of the carotenoid within biological membranes [34]) that influence the profile of antioxidant behaviour displayed by carotenoids, but it is likely that the importance of oxygen addition to carotenoid radicals will be a significant influencing factor. We suggest that the rate constants we have reported will be useful in modelling and accounting for the antioxidant behaviour displayed by carotenoids.

Conclusions

The rate constants for oxygen addition to various carotenoid radicals have been determined and these display a moderate dependence on the conjugated chain length. For reasons of spectral overlap of the absorption of the carotenoid radicals and the parent carotenoid, it has not been possible to extract information relating to the reversibility of the oxygen addition reaction.

Acknowledgements

The authors are grateful to the Leverhulme Trust (Research Grant F/00130F) for financial support and to DSM Nutritional Products for supplying the carotenoids used in this work.

References

[1] El-Agamey A, McGarvey DJ. First direct observation of reversible oxygen addition to a carotenoid-derived carbon-centered neutral radical. Org Lett 2005;7:3957–3960.

[2] El-Agamey A, McGarvey DJ. Evidence for a lack of reactivity of carotenoid addition radicals towards oxygen: A laser flash photolysis study of the reactions of carotenoids with acylperoxyl radicals in polar and non-polar solvents. J Am Chem Soc 2003;125:3330–3340.

[3] Gao Y, Webb S, Kispert LD. Deprotonation of carotenoid radical cation and formation of a didehydrodimer. J Phys Chem B 2003;107:13237–13240.

[4] Woodall AA, Lee SWM, Weesie RJ, Jackson MJ, Britton G. Oxidation of carotenoids by free radicals: Relationship between structure and reactivity. Biochim Biophys Acta 1997;1336:33–42.

[5] D'Aquino M, Dunster C, Willson RL. Vitamin A and glutathione-mediated free radical damage: Competing reactions with polyunsaturated fatty acids and vitamin C. Biochem Biophys Res Commun 1989;161:1199–1203.

[6] Everett SA, Dennis MF, Patel KB, Maddix S, Kundu SC, Willson RL. Scavenging of nitrogen dioxide, thiyl, and sulfonyl free radicals by the nutritional antioxidant β-carotene. J Biol Chem 1996;271:3988–3994.

[7] Mortensen A, Skibsted LH, Sampson J, Rice-Evans C, Everett SA. Comparative mechanisms and rates of free radical scavenging by carotenoid antioxidants. FEBS Lett 1997;418:91–97.

[8] El-Agamey A, McGarvey DJ. Carotenoid addition radicals do not react with molecular oxygen: Aspects of carotenoid reactions with acylperoxyl radicals in polar and non-polar media. Free Radic Res 2002;36(Suppl. S):97–100.

[9] Frenette M, Aliaga C, Font-Sanchis E, Scaiano JC. Bond dissociation energies for radical dimers derived from highly stabilized carbon-centered radicals. Org Lett 2004;6:2579–2582.

[10] Font-Sanchis E, Aliaga C, Cornejo R, Scaiano JC. Reactivity toward oxygen of isobenzofuranyl radicals: Effect of nitro group substitution. Org Lett 2003;5:1515–1518.

[11] Font-Sanchis E, Aliaga C, Focsaneanu KS, Scaiano JC. Greatly attenuated reactivity of nitrile-derived carbon-centered radicals toward oxygen. Chem Commun 2002;1576–1577.

[12] Bejan EV, Font-Sanchis E, Scaiano JC. Lactone-derived carbon-centered radicals: Formation and reactivity with oxygen. Org Lett 2001;3:4059–4062.

[13] Scaiano JC, Martin A, Yap GPA, Ingold KU. A carbon-centered radical unreactive toward oxygen: Unusual radical stabilization by a lactone ring. Org Lett 2000;2:899–901.

[14] Burton GW, Ingold KU. β-Carotene: An unusual type of lipid antioxidant. Science 1984;224:569–573.

[15] Tinkler JH, Tavender SM, Parker AW, McGarvey DJ, Mulroy L, Truscott TG. Investigation of carotenoid radical cations and triplet states by laser flash photolysis and time-resolved resonance Raman spectroscopy: Observation of competitive energy and electron transfer. J Am Chem Soc 1996;118:1756–1761.

[16] Ito O. Reactions of aromatic thiyl radicals. In: Alfassi ZB, editor. S-Centered radicals. Chichester: John Wiley & Sons; 1999. p 193–224.

[17] Britton G. UV/visible spectroscopy. In: Britton G, Liaaen-Jensen S, Pfander H, editors. Carotenoids. Volume 1B: Spectroscopy. Basel: Birkhäuser Verlag; 1995. p 13–62.

[18] Neta P, Huie RE, Ross AB. Rate constants for reactions of peroxyl radicals in fluid solutions. J Phys Chem Ref Data 1990;19:413–513.

[19] Pratt DA, Mills JH, Porter NA. Theoretical calculations of carbon-oxygen bond dissociation enthalpies of peroxyl radicals formed in the autoxidation of lipids. J Am Chem Soc 2003;125:5801–5810.

[20] Tallman KA, Pratt DA, Porter NA. Kinetic products of linoeate peroxidation: Rapid β-fragmentation of nonconjugated peroxyls. J Am Chem Soc 2001;123:11827–11828.

[21] Porter NA, Caldwell SE, Mills KA. Mechanisms of free-radical oxidation of unsaturated lipids. Lipids 1995;30:277–290.

[22] Porter NA, Mills KA, Carter RL. A mechanistic study of oleate autoxidation: Competing peroxyl H-atom abstraction and rearrangement. J Am Chem Soc 1994;116:6690–6696.

[23] Krinsky NI, Yeum K-J. Carotenoid-radical interactions. Biochem Biophys Res Commun 2003;305:754–760.

[24] El-Agamey A, Lowe GM, McGarvey DJ, Mortensen A, Phillip DM, Truscott TG, Young AJ. Carotenoid radical chemistry and antioxidant/pro-oxidant properties. Arch Biochem Biophys 2004;430:37–48.

[25] Edge R, McGarvey DJ, Truscott TG. The carotenoids as anti-oxidants–a review. J Photochem Photobiol B: Biol 1997;41:189–200.

[26] Martin HD, Jäger C, Ruck C, Schmidt M, Walsh R, Paust J. Anti- and prooxidant properties of carotenoids. J Prakt Chem 1999;341:302–308.

[27] Rice-Evans CA, Sampson J, Bramley PM, Holloway DE. Why do we expect carotenoids to be antioxidants *in vivo*? Free Radic Res 1997;26:381–398.

[28] Kennedy TA, Liebler DC. Peroxyl radical scavenging by β-carotene in lipid bilayers. J Biol Chem 1992;267:4658–4663.

[29] Palozza P. Prooxidant actions of carotenoids in biologic systems. Nutr Rev 1998;56:257–265.

[30] Palozza P, Luberto C, Calviello G, Ricci P, Bartoli GM. Antioxidant and prooxidant role of β-carotene in murine normal and tumor thymocytes: Effects of oxygen partial pressure. Free Radic Biol Med 1997;22:1065–1073.

[31] Tsuchihashi H, Kigoshi M, Iwatsuki M, Niki E. Action of β-carotene as an antioxidant against lipid peroxidation. Arch Biochem Biophys 1995;323:137–147.

[32] Tesoriere L, D'Arpa D, Re R, Livrea MA. Antioxidant reactions of all-trans retinol in phospholipid bilayers: Effect of oxygen partial pressure, radical fluxes, and retinol concentration. Arch Biochem Biophys 1997;343:13–18.

[33] Vile GF, Winterbourn CC. Inhibition of adriamycin-promoted microsomal lipid peroxidation by β-carotene, α-tocopherol and retinol at high and low oxygen partial pressures. FEBS Lett 1988;238:353–356.

[34] Young AJ, Lowe GM. Antioxidant and prooxidant properties of carotenoids. Arch Biochem Biophys 2001;385:20–27.